Three-dimensional profilometry with nearly focused binary phase-shifting algorithms

Laura Ekstrand and Song Zhang*

Department of Mechanical Engineering, Iowa State University, Ames, Iowa 50011, USA
Corresponding author: song@iastate.edu

This Letter investigates the effects of different phase-shifting algorithms on the quality of high-resolution three-dimensional (3-D) profilometry produced with nearly focused binary patterns. From theoretical analyses, simulations, and experiments, we found that the nine-step phase-shifting algorithm produces accurate 3-D measurements at high speed without the limited depth range and calibration difficulties that typically plague binary defocusing methods. We also found that the use of more fringe patterns does not necessarily enhance measurement quality.   © 2011 Optical Society of America
OCIS codes: 120.0120, 120.2650, 100.5070.

Three-dimensional (3-D) profilometry based on digital sinusoidal fringe projection techniques has seen great success in both scientific studies and industrial practices [1]. However, it remains challenging to perform high-quality 3-D profilometry with off-the-shelf digital video projectors, especially due to their nonlinear gamma.

The binary defocusing technique [2] can circumvent this nonlinear gamma problem. Similar to the method of Su *et al.* using a Ronchi grating [3], this approach strives to generate ideal sinusoidal fringe patterns by defocusing binary structured ones. However, compared to the conventional sinusoidal fringe generation technique, this technique has two major shortcomings: a smaller depth-measurement range [4] and the difficulty of calibrating the defocused projector [2].

If, rather than defocusing binary patterns to resemble ideal sinusoids, a 3-D profilometry system could employ the patterns in their nearly focused state (i.e., with strong binary structures still evident), the depth range could closely resemble that of the conventional sinusoidal fringe generation technique. Moreover, since traditional, highly accurate calibration methods tolerate minor deviations from absolute focus, such a nearly focused system, if successful, could employ these calibration methods to produce 3-D measurements of high accuracy. In this endeavor, Ayubi *et al.* [5] proposed modulating the squared binary structured patterns with sinusoidal pulse width modulation to shift the harmonics far away from the fundamental frequency. Thus, even slight deviations from focus (similar to low-pass filtering) could neutralize the harmonics and generate high-quality sinusoidal patterns. Wang and Zhang [6] proposed the optimal pulse width modulation (OPWM) technique to further advance this method. The OPWM technique selectively eliminates the error-causing harmonics of a squared binary pattern by making notches in the pattern. Both methods can significantly improve the measurement quality when the fringe stripes are wide. However, their influence is minimized when the fringe stripe is narrow because of the discrete fringe generation nature. Ayubi *et al.* proposed another method that uses separate binary images to represent each bit in an 8 bit grayscale sinusoidal pattern [7]. However, it requires at least eight images to generate each high-quality sinusoidal one, which reduces the

measurement speed by 1/8. Zhang proposed the subdivision of each phase-shifting algorithm step into four substeps [8]. Averaging each set of four back into a whole step prior to calculating the phase effectively cancels the phase error due to the harmonics below the seventeenth order. The remaining harmonics impart error that is negligible for most applications in comparison with the system quantization error. However, the subdivision method still slows down the measurement by a factor of 4. Therefore, the adoption of nearly focused binary techniques requires the improvement of measurement accuracy without sacrificing speed.

In this endeavor, this Letter investigates the effects of utilizing different phase-shifting algorithms on the quality of 3-D profilometry produced with nearly focused binary patterns. Theoretical analyses, simulations, and experiments will be presented to demonstrate the performance of three- to nine-step phase-shifting algorithms.

In general, an N-step phase-shifting algorithm with equal phase shifts can be described as

$$I_n(x,y) = I'(x,y) + I''(x,y)\cos(\phi + 2\pi n/N), \quad (1)$$

where $I'(x,y)$ is the average intensity, $I''(x,y)$ the intensity modulation, $\phi(x,y)$ the phase to be solved for, and $n = 1, 2, \ldots, N$. Solving these equations leads to

$$\phi(x,y) = \tan^{-1}\frac{\sum_{n=1}^{N} I_n(x,y)\sin(2\pi n/N)}{\sum_{n=1}^{N} I_n(x,y)\cos(2\pi n/N)}. \quad (2)$$

The phase obtained in Eq. (2) ranges from $-\pi$ to $+\pi$ with 2π discontinuities. A phase-unwrapping algorithm such as that in [9] can be used to obtain the continuous phase, which can be converted to 3-D shape data if the system is calibrated.

For fringe patterns that are not ideally sinusoidal, such as nearly focused binary patterns, Eq. (2) will not yield the correct phase. Unlike ideal sinusoids, which have one fundamental frequency, binary structured patterns (essentially square waves) have numerous harmonics which cause phase error. In general, the normalized square wave with a period of 2π can be described as

$$y(x) = \begin{cases} 0 & x \in [(2n-1)\pi, 2n\pi) \\ 1 & x \in [2n\pi, (2n+1)\pi) \end{cases}. \qquad (3)$$

Here n is an integer number. The square wave can be expanded as a Fourier series,

$$y(x) = 0.5 + \sum_{k=0}^{\infty} \frac{2}{(2k+1)\pi} \sin[(2k+1)x]. \qquad (4)$$

To understand how each harmonic frequency component affects the measurement quality, we analyze its associated phase error. Using Eq. (2), we compute the base phase $\phi^b(x,y)$ obtained from the fundamental frequency. Then we compute the erroneous phase $\phi^k(x,y)$ obtained from the combination of the fundamental frequency and the particular harmonic component under study. The fringe patterns with an added $(2k+1)$th-order harmonic component can be written as

$$I_n^k = I' + I''[\cos\gamma + \cos(M\gamma)/M]. \qquad (5)$$

Here $\gamma = \phi + 2\pi n/N$ and $M = 2k+1$. Using the fringe patterns $I_n^k(x,y)$ in Eq. (2) will yield $\phi^k(x,y)$. The phase error is then defined as

$$\Delta\phi^k(x,y) = \phi^k(x,y) - \phi^b(x,y). \qquad (6)$$

Table 1 summarizes the theoretical phase errors caused by different orders of harmonics for each phase-shifting algorithm. A couple key trends can be observed in the data. First, the algorithms with odd numbers of steps experience much less error from the harmonics than algorithms with even numbers of steps. Second, the nine-step algorithm does not experience any error from harmonics below the seventeenth order. Therefore, it theoretically achieves at least the same accuracy as the method proposed in [8] with only nine fringe patterns instead of 12, increasing the measurement speed by 25%.

Simulations were conducted to analyze the performance of different phase-shifting algorithms. We first simulated the random noise effect. The square was smoothed by a five-pixel Gaussian filter with a standard deviation, $\sigma = 0.83$ pixels to simulate an imperfect projector focus. A fringe period of $P = 38$ was chosen to ensure that each had some phase-shift error. Random noise with different power was also added to show

Table 1. Phase Errors Caused by Different Harmonics for Different Phase-Shifting Algorithms[a]

Step N	Order of Harmonics M						
	3	5	7	9	11	13	15
3	0.00	0.14	0.10	0.00	0.06	0.05	0.00
4	0.24	0.14	0.10	0.08	0.06	0.05	0.05
5	0.00	0.00	0.00	0.08	0.06	0.00	0.00
6	0.00	0.14	0.10	0.00	0.06	0.05	0.00
7	0.00	0.00	0.00	0.00	0.00	0.05	0.05
8	0.00	0.00	0.10	0.08	0.00	0.00	0.05
9	0.00	0.00	0.00	0.00	0.00	0.00	0.00

[a]This table shows the rms phase errors in radians for fringe period $P = 60$ pixels.

Table 2. Phase Errors Caused by Random Noise

Noise	$N = 3$	$N = 4$	$N = 5$	$N = 6$	$N = 7$	$N = 8$	$N = 9$
10 dB	0.27	0.39	0.16	0.23	0.13	0.17	0.11
20 dB	0.21	0.36	0.09	0.20	0.06	0.13	0.05
30 dB	0.20	0.36	0.09	0.20	0.05	0.13	0.05
40 dB	0.20	0.36	0.08	0.20	0.05	0.12	0.05
None	0.20	0.36	0.08	0.20	0.05	0.12	0.05

Table 3. Phase Errors with Different Fringe Widths[a]

Period	$N = 3$	$N = 4$	$N = 5$	$N = 6$	$N = 7$	$N = 8$	$N = 9$
36	0.19	0.35	0.08	0.19	0.05	0.12	0.01
42	0.21	0.37	0.09	0.20	0.03	0.13	0.04
48	0.22	0.37	0.10	0.22	0.06	0.14	0.04
54	0.23	0.39	0.11	0.23	0.06	0.15	0.03

[a]Gaussian filter, FS = 5, $\sigma = 0.83$ pixel; noise, 30 dB.

their influence. The phase errors for the different phase-shifting algorithms were computed relative to ideal sinusoidal fringe results. Table 2 summarizes the results. It shows that, when the noise is reduced to 40 dB, the noise effect is not vivid.

Different fringe periods were also used to show phase-shift error effect, as summarized in Table 3. This simulation shows that, when $P = 42$, the seven-step algorithm outperforms the nine-step algorithm since it does not have phase-shift error; and when $P = 36$, the phase error for the nine-step algorithm is only rms $0.15\% = 0.01/(2\pi)$. This is smaller than the quantization error of an 8 bit camera ($1/2^8 \approx 0.39\%$).

Moreover, we simulated the influence of different amounts of defocusing by changing the filter size (FS) while ensuring the standard deviation of $\sigma = 1/6$ FS. Table 4 presents the results. In this simulation, fringe period of $P = 42$ was used to ensure that no phase-shift error for the seven-step algorithm. This simulation shows that, when the FS increases (i.e., fringe pattern becomes more and more sinusoidal), the phase errors decrease for all algorithms, and when the FS is large enough, most algorithms result in small measurement error with odd-number phase-shifting algorithms being better.

Experiments were also carried out to verify the performance of the different algorithms. The hardware system is composed of a CCD camera (Pulnix TM6740-CL) and a digital-light-processing projector (Samsung SP-P310MEMX). The camera uses a 16 mm focal length lens (Computar M1614-MP). The projector and the camera remained untouched between experiments.

We first measured a uniform white board with fringe period $P = 38$. Figure 1 shows the results for comparison. One of the fringe patterns is illustrated in Fig. 1(a)

Table 4. Phase Errors with Different Defocusing Degrees[a]

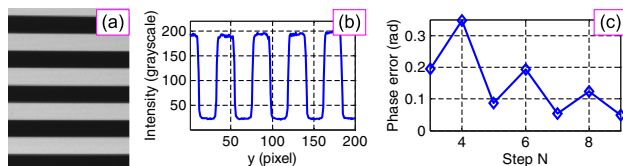| FS	$N = 3$	$N = 4$	$N = 5$	$N = 6$	$N = 7$	$N = 8$	$N = 9$
9	0.11	0.28	0.04	0.11	0.01	0.06	0.02
13	0.05	0.20	0.03	0.05	0.01	0.04	0.01
17	0.02	0.14	0.03	0.02	0.01	0.03	0.01

[a]Fringe period, $P = 42$; noise, 30 dB.

Fig. 1.   (Color online) Measurement results for a flat board using different phase-shifting algorithms. (a) One of the fringe patterns. (b) Cross section of the fringe pattern. (c) The rms errors are 0.19, 0.35, 0.08, 0.19, 0.05, 0.12, and 0.05 rad for three-, four-, five-, six-, seven-, eight-, and nine-step algorithms, respectively.
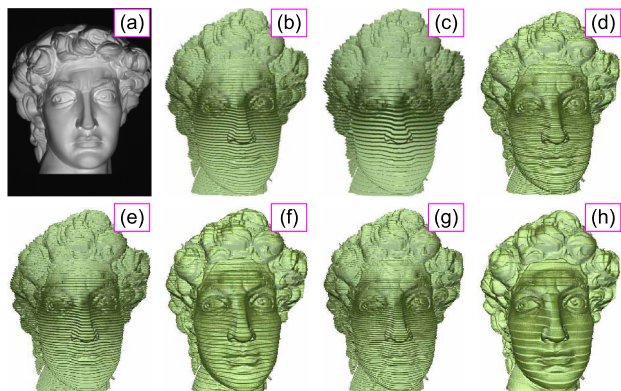

Fig. 2.   (Color online) Experimental results of different binary phase-shifting algorithms with a nearly focused projector. (a) Photograph of the captured statue. (b), (c), (d), (e), (f), (g), (h) 3-D results of the three-, four-, five-, six-, seven-, eight-, and nine-step algorithms, respectively.
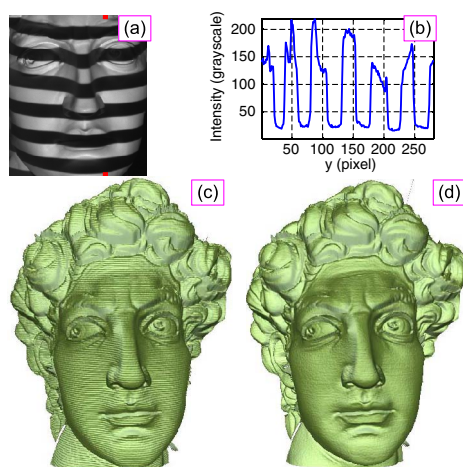

Fig. 3.   (Color online) Experimental results without phase-shift error under the same defocusing degree as Fig. 2. (a)–(b) Close-up view of one of the binary patterns and its 210th column cross section (indicated by red squares). (c) 3-D result by the seven-step algorithm ($P = 42$). (d) 3-D result by the nine-step algorithm ($P = 36$).

whose cross section is shown in Fig. 1(b). It clearly shows binary structures. The phase errors of the different algorithms, computed as in [4], are plotted in Fig. 1(c); they agree with our simulation results. This experiment further verifies that a seven- or nine-step algorithm only results in very small phase error, thus enabling relatively accurate 3-D measurement.

A more complex 3-D statue (approximately $190\,\mathrm{mm}\,W \times 419\,\mathrm{mm}\,H \times 165\,\mathrm{mm}\,D$) was also measured with the different phase-shifting algorithms. Figure 2 shows the measurement results. This experiment indicates that, when the projector is nearly focused, the seven- and nine-step algorithms yield the most accurate results, while the four-step algorithm yields the least accurate results. Again, $P = 38$ was used as a basis for comparison to ensure that all the algorithms had some phase-shift error.

To illustrate the best results without phase-shift errors, we used $P = 42$ with a seven-step algorithm and 36 with a nine-step algorithm. Figure 3 presents the results. The results clearly indicate a nine-step algorithm and a nearly focused projector for accurate 3-D measurement.

In addition, we evaluated the system accuracy by measuring a known step-height (50 mm) object and compared the measurement result against the result obtained from the conventional fringe projection technique with the projector's nonlinear gamma being corrected. The difference between these two results is less than rms 0.3%. This further validated the success of the nine-step algorithm with nearly focused binary patterns.

This Letter has demonstrated that phase-shifting algorithm selection has a dramatic effect on the quality of 3-D profilometry with nearly focused binary patterns. Our results show that the nine-step binary phase-shifting algorithm has the potential to rapidly perform high-quality measurement with a nearly focused projector, giving it a significantly larger depth range and more accurate calibration than the typical defocusing technique.

References

1. G. Geng, Adv. Opt. Photon. **3**, 128 (2011).
2. S. Lei and S. Zhang, Opt. Lett. **34**, 3080 (2009).
3. X. Y. Su, W. S. Zhou, G. von Bally, and D. Vukicevic, Opt. Commun. **94**, 561 (1992).
4. Y. Xu, L. Ekstrand, J. Dai, and S. Zhang, Appl. Opt. **50**, 2572 (2011).
5. G. A. Ayubi, J. A. Ayubi, J. M. D. Martino, and J. A. Ferrari, Opt. Lett. **35**, 3682 (2010).
6. Y. Wang and S. Zhang, Opt. Lett. **35**, 4121 (2010).
7. G. A. Ayubi, J. M. D. Martino, J. R. Alonso, A. Fernandez, C. D. Perciante, and J. A. Ferrari, Appl. Opt. **50**, 147 (2011).
8. S. Zhang, Appl. Opt. **50**, 1753 (2011).
9. S. Zhang, X. Li, and S.-T. Yau, Appl. Opt. **46**, 50 (2007).